

Piperazine and piperidine carboxamides and carbamates as inhibitors of fatty acid amide hydrolase (FAAH) and monoacylglycerol lipase (MAGL)

Jani Korhonen^a, Anne Kuusisto^a, John van Bruchem^a, Jayendra Z. Patel^a, Tuomo Laitinen^a, Dina Navia-Paldanius^b, Jarmo T. Laitinen^b, Juha R. Savinainen^b, Teija Parkkari^a, Tapio J. Nevalainen^{a,*}

^a School of Pharmacy, Faculty of Health Sciences, University of Eastern Finland, PO Box 1627, FIN-7021 Kuopio, Finland

^b School of Medicine, Institute of Biomedicine, University of Eastern Finland, PO Box 1627, FIN-7021 Kuopio, Finland

ARTICLE INFO

Article history:

Received 30 June 2014

Accepted 5 September 2014

Available online 16 September 2014

Keywords:

Fatty acid amide hydrolase (FAAH)

Monoacylglycerol lipase (MAGL)

FAAH and MAGL inhibitors

ABSTRACT

The key hydrolytic enzymes of the endocannabinoid system, fatty acid amide hydrolase (FAAH) and monoacylglycerol lipase (MAGL), are potential targets for various therapeutic applications. In this paper, we present more extensively the results of our previous work on piperazine and piperidine carboxamides and carbamates as FAAH and MAGL inhibitors. The best compounds of these series function as potent and selective MAGL/FAAH inhibitors or as dual FAAH/MAGL inhibitors at nanomolar concentrations. This study revealed that MAGL inhibitors should comprise leaving-groups with a conjugate acid pK_a of 8–10, while diverse leaving groups are tolerated for FAAH inhibitors.

© 2014 Elsevier Ltd. All rights reserved.

1. Introduction

Endocannabinoids, *N*-arachidonylethanolamine (AEA) and 2-arachidonoylglycerol (2-AG) have been found in most mammalian tissues and they stimulate cannabinoid CB1 and CB2 receptor activity thereby modulating several physiological responses, including nociception, anxiety, and depression.^{1,2} The two main enzymes involved in endocannabinoid degradation are monoacylglycerol lipase (MAGL) and fatty acid amide hydrolase (FAAH). Two additional endocannabinoid-hydrolyzing enzymes have recently been discovered: α/β -hydrolase domain containing serine hydrolases ABHD6 and ABHD12, which are described as complementary 2-AG-degrading enzymes in the brain.³ Inhibition of these enzymes leads to accumulation of endocannabinoids and inducement of cannabinomimetic effects.⁴

FAAH is the primary AEA-degrading enzyme,⁵ but it is also capable of hydrolyzing other bioactive *N*-acylethanolamines (NAEs), such as *N*-palmitoylethanolamine (PEA),⁶ *N*-oleoylethanolamine (OEA)⁶ and the sleep-inducing lipid oleamide.⁷

Pharmacological inhibition of FAAH has been considered as potential therapeutic approach for the treatment of several nervous system disorders, including pain, inflammation, anxiety, and depression.^{2,8,9}

MAGL inhibitors may have therapeutic potential in treatment of cancer and neuroinflammatory diseases. MAGL hydrolyzes 2-AG to arachidonic acid, from which cyclooxygenases can synthesize neuroinflammatory prostaglandins.¹⁰ Therefore, it is possible that inhibition of MAGL may be an alternative way to regulate prostaglandin production and to reduce inflammation in neurodegenerative diseases. In addition, MAGL has been shown to control lipid metabolism in cancer cells by promoting production of lipid molecules towards oncogenic lipid messengers.¹¹

A large number of FAAH inhibitors have been described over the years, such as α -keto heterocycles, lactams, carbamates, and piperidine/piperazine based ureas.¹² So far, the most promising irreversible FAAH inhibitors with respect to selectivity and potency are piperidine and piperazine urea compounds, such as PF-3845 and JNJ-1661010 (Fig. 1). The development of potent and selective MAGL inhibitors has been slower compared to that of FAAH due to only recent availability of X-ray crystal structural data.^{13–15} In the model by Sanofi-Aventis, the crystal structure of MAGL was built by complexing the enzyme with the piperazine triazole urea inhibitor SAR629.¹⁴ This structure was one starting point for our compound series of piperazine triazole urea compounds. Very recently, remarkable progress has been achieved in the discovery of potent and selective MAGL inhibitors. Cravatt and co-workers have reported MAGL selective piperidine carbamate based inhibitors JZL184 and KLM-29 and piperazine carbamate based dual FAAH–MAGL inhibitors, such as JZL195 (Fig. 1). Other very recently published piperidine/piperazine ureas are benzotriazol-1-yl

* Corresponding author. Tel.: +358 40 355 2479.

E-mail address: tapio.nevalainen@uef.fi (T.J. Nevalainen).

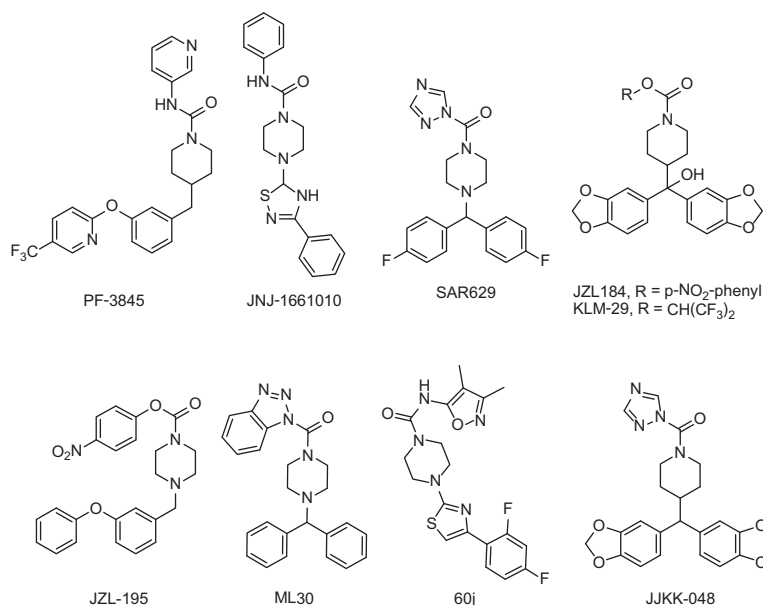


Figure 1. Structures of FAAH and MAGL inhibitors.

carboxamides, such as ML30 (Fig. 1) by Lambert and co-workers¹⁶ and piperazine ureas (e.g., 60j) by Kono et al.^{17,18} While writing this manuscript, Wilson and co-workers have reported radiosynthesis of carbamate- and urea-based MAGL inhibitors.¹⁹

In this work, we follow up our previous study, in which we have designed and characterized piperazine and piperidine triazole ureas as highly potent and MAGL-selective inhibitors culminating in the synthesis of JJKK-048, which appeared the most potent and MAGL selective inhibitor currently described ($IC_{50} < 0.4$ nM).²⁰ Here, we describe the further optimization of piperazine and piperidine carboxamides and carbamates as potent and selective MAGL/FAAH inhibitors or as dual FAAH/MAGL inhibitors.

2. Chemistry

(Benzhydrylpiperazin-1-yl)carboxamides **3a–f** were synthesized by triphosgene-mediated coupling of benzhydrylpiperazine **1** with either with the appropriate aniline or heterocyclic amine (Scheme 1). Compounds **3g–h** were synthesized as shown in Scheme 1 starting by carbamylation of the heterocyclic amines with phenyl (**4a**) or *p*-nitrophenyl chloroformate (**4b**) to give the phenyl carbonyl derivatives **5a–b**. Subsequent urea formation of **5a–b** with **1** yielded **3g–h**.

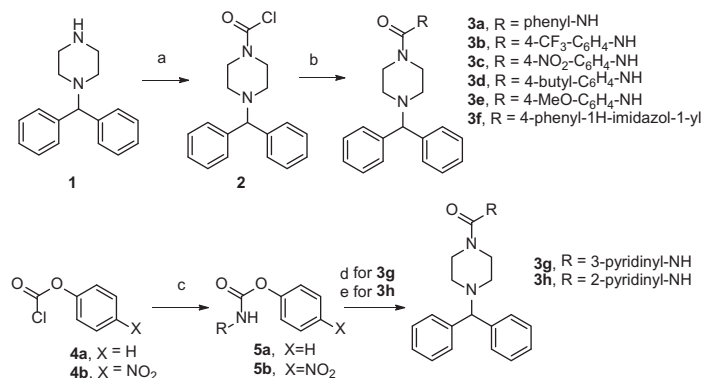
The urea derivatives **7a–e** were obtained from 1-(3-phenoxybenzyl)-piperazine (**6**)²⁰ by reaction of isocyanate, or triphosgene

and subsequent reaction of produced carbonyl chloride with the amine RH as shown in Scheme 2. The imidazole urea **7g** was prepared by reaction of **6** with 1,1'-carbonyldiimidazole. *O*-hexafluoroisopropyl (HFIP) carbamate **7f** (JW642) was synthesized by the reaction of hexafluoroisopropyl chloride, generated by treatment of hexafluoroisopropanol with triphosgene, with **6**.

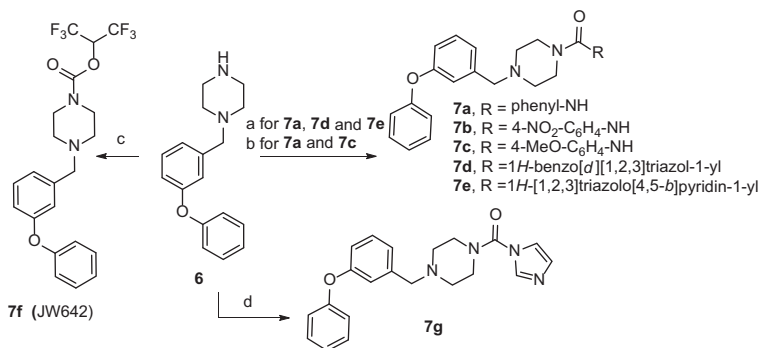
The 4-phenoxybenzyl carbamate **9a** (JJKK-011) was made by carbamylation of 1-(4-phenoxybenzyl)-piperazine (**8**)²⁰ with 4-nitrophenyl chloroformate and urea analogs **9b–c** were prepared by microwave assisted synthesis from **8** coupling with 1,1'-carbonyldiimidazole (CDI) and 1,1'-carbonylbis-benzotriazole,²¹ respectively, as shown in Scheme 3.

4-(Bis(3,4-dioxymethylenephényl)methyl and -methylene derivatives **11a–b** were obtained by carbamylation of piperidine derivatives **10a–b**²⁰ with 4-nitrophenyl chloroformate as shown in Scheme 4.

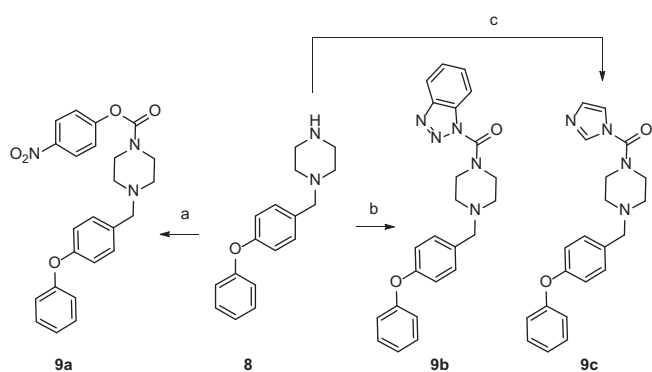
The 4-bisarylcbinol derivatives **12b–c** (TP-TK-042, JJKK-053) were prepared from 4-(bis(3,4-dioxymethylene phenyl)hydroxymethyl)piperidine (**15**, TP-TK-038) coupling with 1,1'-carbonyl-di-(1,2,4-triazole) (CDT) and 2,2,2-trichloroethyl chloroformate, respectively, as shown in Scheme 5. The intermediate **15** was synthesized starting from ethyl isonipecotate **13**. In a first step **13** was protected with CbzCl to yield 1-benzyl 4-ethyl piperidine-1,4-dicarboxylate (**14**). In the following step, lithiation of 1-bromo-3,4-(methylenedioxy)benzene at -78 °C with *t*-BuLi and subsequent



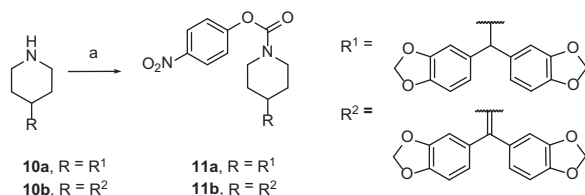
Scheme 1. Synthesis of benzhydrylpiperazin-1-yl)carboxamides **3a–h**. Reagents and conditions: (a) triphosgene, pyridine, CH₂Cl₂, -5 °C; (b) amine RH; DMAP, DIPEA, THF, RT; (c) amine; DMAP, Et₃N, MeCN, RT; (d) **1**, MeCN, pyridine, refl. 2.5 h; (e) **1**, MeCN, pyridine, microwaves, 120 °C, 15 min.



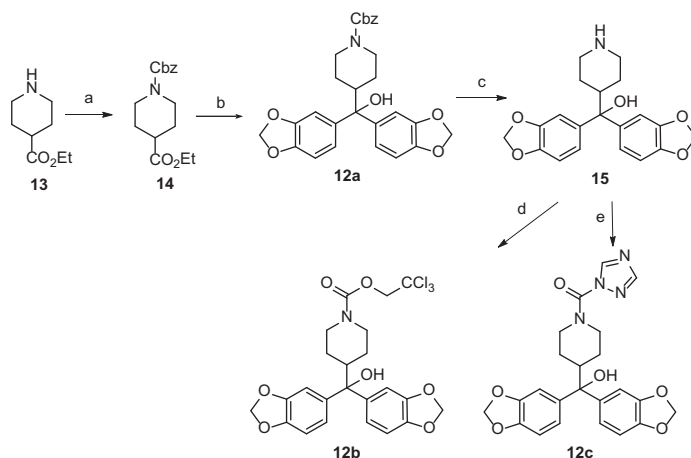
Scheme 2. Synthesis of 3-phenoxyphenylpiperazine ureas **7a–g**. Reagents and conditions: (a) RNCO, THF, 80 °C; (b) triphosgene, pyridine, CH₂Cl₂ 0 °C and then amine RH, DMAP, DIPEA, THF, 0 °C to RT or RT; (c) triphosgene, DIPEA, CH₂Cl₂, 0 °C to RT and then (CF₃)₂CHOH, 0 °C; (d) CDI, DIPEA, THF, 0 °C to RT.



Scheme 3. Synthesis of 4-phenoxyphenylpiperazine ureas **9a–c**. Reagents and conditions: (a) 4-NO₂PhCOCl, DIPEA, CH₂Cl₂; (b) 1,1'-carbonylbisbenzotriazole, THF, microwaves, 130 °C; (c) CDI, THF, microwaves, 4 h, 80–120 °C.



Scheme 4. Synthesis of 4-nitrophenyl carbamates **11a–b**. Reagents and conditions: (a) 4-NO₂PhCOCl, Et₃N, CH₂Cl₂; RT.



Scheme 5. Synthesis of 4-bisarylcarbinol derivatives **12b–c**. Reagents and conditions: (a) CbzCl; Et₃N, CHCl₃, 0 °C to RT; (b) toluene, BuLi, –78 °C and then 4-bromo-1,2-methylenedioxybenzene, –78 °C to RT; (c) H₂, Pd/C; (d) CCl₃CH₂OCOCI, CH₂Cl₂, Et₃N, RT; (e) CDT, THF, DIPEA, RT.

reaction with **14** gave Cbz-protected piperidine **12a**. Finally, elimination of the Cbz group by hydrogenation afforded the piperidinealcohol **15**.

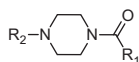
3. Results and discussion

3.1. Benzhydryl-, phenyl- and ethoxycarbonylpiperazine derivatives

In the previous paper, we demonstrated that SAR629, the covalent inhibitor co-crystallized with MAGL¹⁴ and its close structural analog AKU-005, inhibited MAGL activity with subnanomolar potencies (IC₅₀ values 0.2–1.1 nM).²⁰ As the IC₅₀ values towards FAAH were not reported in our previous paper, we present here inhibition results of human recombinant FAAH (hrFAAH) accompanied by MAGL inhibition data (Table 1). We demonstrated previously, that the replacement of the triazole moiety with *p*-nitrophenoxy resulted in >1000-fold loss of MAGL inhibitor potency, as shown for AKU-015 and AKU-003. The same trend can be seen for FAAH inhibition, where no inhibition of FAAH could be detected at 10 μM concentration with the *p*-nitrophenoxy analogs AKU-015 and AKU-003, which had only a modest inhibitory activity against MAGL. Triazolopyridine analog AKU-002 was almost as potent as triazole analog AKU-005 inhibiting both FAAH and MAGL. MAGL inhibitor potency was dramatically reduced by replacing triazole with imidazole (AKU-004), whereas the effect against FAAH was not so significant: AKU-004 was only five-fold less active than AKU-005. Reduction of MAGL inhibitor potency was observed by substituting the bulky benzhydryl moiety with

Table 1

MAGL and FAAH inhibitor potencies of benzhydryl-, phenyl and ethoxycarbonylpiperazine derivatives. Results are from two independent experiments performed in duplicate (variability?).



Compd	R ₁	R ₂	-log IC ₅₀ (range) [IC ₅₀ nM]	
			hrMAGL ^a	hrFAAH ^b
SAR629		(4-FPh) ₂ CH	9.07 (9.05–9.10) [0.9]	6.55 (6.54–6.56) [282]
AKU-015		(4-FPh) ₂ CH	6.46 (6.31–6.60) [347]	85 (84–86) ^c
AKU-005		Ph ₂ CH	8.88 (8.73–9.03) [1.3]	6.35 (6.28–6.41) [452]
AKU-003		Ph ₂ CH	6.59 (6.44–6.74) [257]	86 (86–87) ^c
AKU-002		Ph ₂ CH	8.77 (8.47–9.06) [1.7]	6.01 (5.95–6.07) [971]
AKU-004		Ph ₂ CH	51 (44–58) ^c	5.64 (5.57–5.70) [2300]
AKU-009		Ph	6.56 (6.51–6.61) [275]	7.95 (7.94–7.96) [11]
AKU-010		Ph	6.88 (6.82–6.94) [132]	8.22 (8.19–8.26) [6.0]
AKU-033		CO ₂ Et	5.72 (5.42–6.01) [1905]	6.64 (6.62–6.65) [231]
AKU-034		CO ₂ Et	5.78 (5.57–5.98) [1660]	6.85 (6.83–6.88) [141]

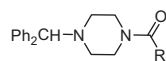
^a Human recombinant MAGL expressed transiently in HEK293 cells.

^b Human recombinant FAAH expressed transiently in COS7 cells.

^c Remaining activity at 10 μM (% control (range) *n* = 2).

Table 2

MAGL and FAAH inhibitor potencies of benzhydrylpiperazine phenyl, pyridinyl-, and pyrimidyl ureas



Compd	R	Remaining activity at 10 μM (% control (range) <i>n</i> = 2)	
		hrMAGL ^a	hrFAAH ^b
3a		62 (45–79)	88 (88–89)
3b		96 (94–98)	86 (83–90)
3c		58 (51–65)	84 (76–92)
3d		92 (85–99)	84 (81–87)
3e		86 (74–97)	89 (83–95)
3f		93 (91–94)	62 (59–65)
3g		101 (93–110)	87 (86–87)
3h		94 (93–95)	87 (86–87)

^{a,b} See footnotes for Table 1.

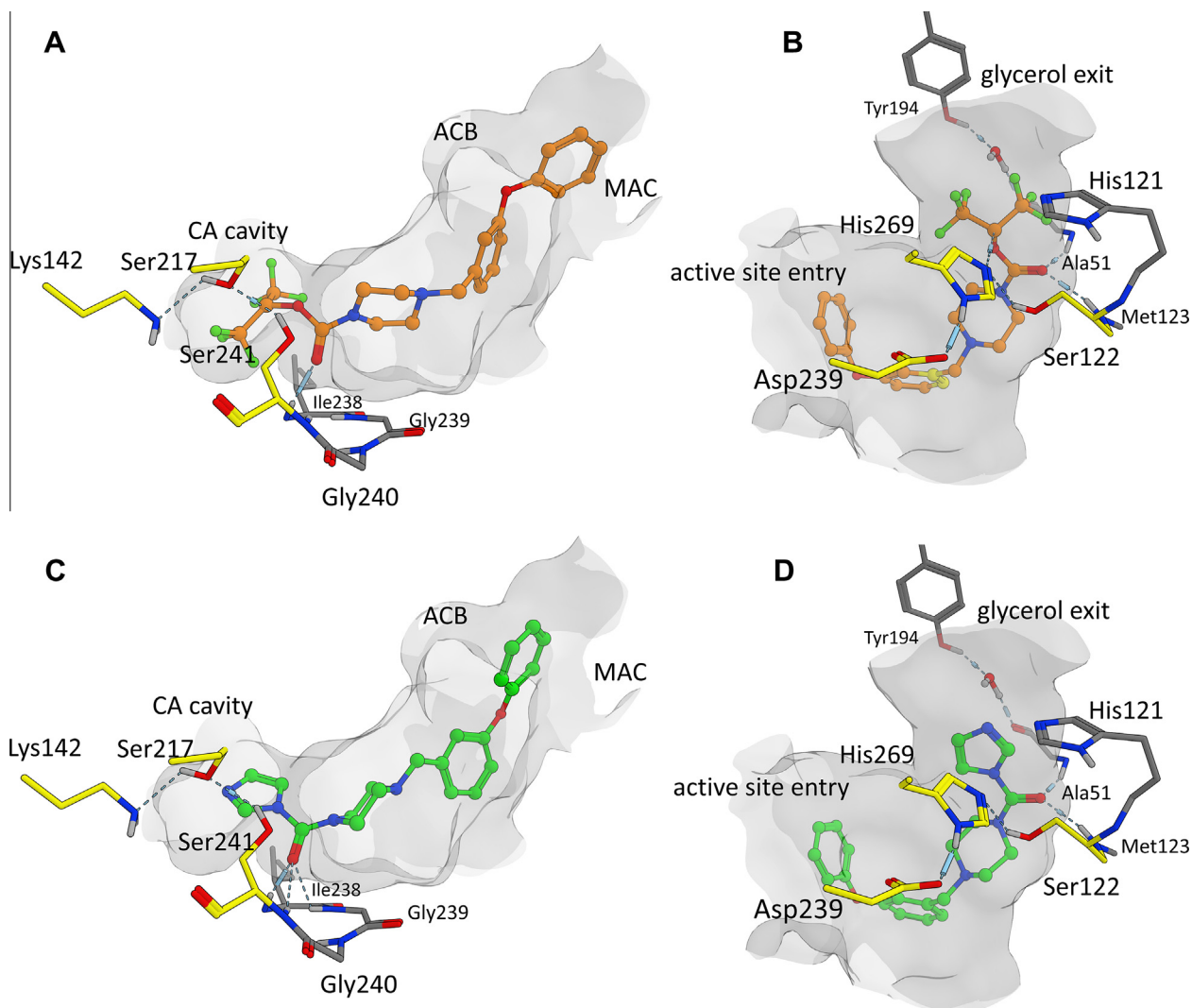


Figure 2. Favorable docking poses inhibitors of compounds **7f** (orange) and **7g** (green) docked to FAAH (panels A and B) and MAGL (panels C and D). Catalytic triad residues (MAGL: Ser122-Asp239-His269; FAAH: Ser241-217-Lys142) are colored using yellow carbons and the residues forming the oxyanion hole (MAGL: Met123 and Ala51; FAAH: Ile238, Gly239, Gly240) are also illustrated. Other residues defining the shape of the cavity are omitted for the clarity and molecular surface is used instead for illustrating the shape cavity shown in light gray. Placement of a conserved water molecule typically found in experimental MAGL structures is shown. (CA = cytosol access, ACB = acyl binding site, MAC = membrane access.)

phenyl (AKU-009 and AKU-010) or ethoxycarbonyl (AKU-033 and AKU-034). In contrast, the FAAH inhibitory activity was not reduced but rather increased. The phenyl analogs (AKU-009 and AKU-010) were potent FAAH inhibitors (IC_{50} 11 and 6 nM, respectively) and demonstrated 75- to 88-fold potency over benzhydryl analogs (AKU-005 and AKU-002). Also ethoxycarbonyl analogs (AKU-033 and AKU-034) were moderately potent (IC_{50} 231 and 141 nM, respectively) and showed 3- to 4-fold potency over benzhydryl analogs (AKU-005 and AKU-002). These results clearly indicate that the benzhydryl substituent on the 4-piperazine position is too bulky to be effective against FAAH, whereas a smaller lipophilic phenyl substituent is favorable, even more favorable than the small but polar ethoxycarbonyl group.

3.2. Benzhydrylpiperazine phenyl-, pyridinyl-, phenylimidazolyl- and pyrimidyl ureas **3a-i**

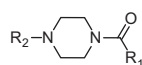
As some of the known potent FAAH inhibitors (e.g., PF-750, PF-3845 and JNJ-1661010) contain a phenyl- or pyridinyl piperidine urea structure, it encouraged us to synthesize corresponding

benzhydrylpiperazine-aryl ureas. We also wanted to find out whether different substituents of the phenyl ring have an effect on the FAAH and MAGL inhibitory activities and therefore, we prepared series of substituted phenyl ureas (**3a-h**) (Table 2). Unfortunately, these derivatives were very poor inhibitors, having 58–89% remaining activity at 10 μ M compound concentration. MAGL inhibitory activity was also lost by introduction of 4-phenylimidazole moiety (**3f**). Practically, none of the compounds showed noticeable FAAH inhibitory activity, except **3f**, which had 62% remaining FAAH activity at 10 μ M concentration. These results indicate that the benzhydrylpiperazine-phenyl-, -phenylimidazolyl-, and -pyridinyl ureas are ineffective inhibitors of both MAGL and FAAH.

3.3. Phenoxyphenyl piperazine derivatives

In a similar manner as for JZL184, we prepared the triazole analogs of dual FAAH-MAGL inhibitor JZL195 by replacing the *p*-nitrophenoxy-moiety with triazole (JJKK-006), phenylamino (**7a**), *p*-nitrophenylamino (**7b**), *p*-methoxyphenylamino (**7c**),

Table 3
MAGL and FAAH inhibitor potencies of phenoxyphenyl piperazine derivatives



Compd	R ₁	R ₂	-logIC ₅₀ (range) [IC ₅₀ nM]	
			hrMAGL ^a	hrFAAH ^b
JJKK-006		3-(PhO)Bn	9.26 (9.03–9.42) [0.6]	8.57 (8.55–8.58) [2.7]
7a		3-(PhO)Bn	98 (97–99) ^c	5.52 (5.49–5.55) [3020]
7b		3-(PhO)Bn	102 (102–102) ^c	98 (97–99) ^c
7c		3-(PhO)Bn	78 (76–80) ^c	56 (54–58) ^c
7d		3-(PhO)Bn	8.11 (8.07–8.15) [7.8]	7.05 (7.04–7.06) [89]
7e		3-(PhO)Bn	8.26 (8.17–8.36) [5.5]	7.64 (7.62–7.66) [23]
7f		3-(PhO)Bn	7.13 (7.11–7.15) [74]	76 (76–76) ^c
7g		3-(PhO)Bn	5.55 (5.52–5.58) [2844]	7.81 (7.77–7.85) [15]
9a		4-(PhO)Bn	5.95 (5.87–6.02) [1100]	43 (40–46) ^c
9b		4-(PhO)Bn	7.16 (7.16–7.17) [70]	6.15 (6.14–6.17) [708]
9c		4-(PhO)Bn	6.18 (6.11–6.25) [660]	7.76 (7.66–7.85) [3.4]

^{a,b} See footnotes for Table 1.

^c Remaining activity at 10 μM (% control (range), n = 2).

benzotriazole (**7d**) and triazolopyridine (**7e**), hexafluoroisopropoxy (**7f**) and imidazole (**7g**) groups (Table 3). As we observed in our previous study,²⁰ the replacement of the *p*-nitrophenoxy group of JZL195 with the triazole moiety (JJKK-006) resulted in a dramatic increase in MAGL inhibitor potency. As expected, the benzotriazole- (**7e**) and triazolopyridine- (**7f**) analogs were somewhat weaker MAGL inhibitors than the corresponding triazole analog.

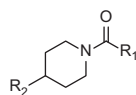
Evidently, the triazole analog JJKK-006 was potent FAAH inhibitor with IC₅₀ value of 2.7 nM, and 4.5-fold selectivity for MAGL over FAAH. Phenylamino (**7a**) and imidazole (**7g**) substituted analogs showed good FAAH inhibitory activity, whereas 4-nitro- and 4-methoxy-substituted aniline ureas (**7b–c**) were ineffective. It seems that steric bulk exerted by the nitro- and methoxy-substituents lead to a loss in activity. As expected, the benzotriazole (**7d**) and triazolopyridine (**7e**) analogs were potent inhibitors of FAAH and MAGL being somewhat weaker than triazole analog JJKK-006 and having 10- and 4-fold selectivity for MAGL over FAAH, respectively.

The *O*-hexafluoroisopropyl (HFIP) carbamate **7f** showed only negligible activity against FAAH at 10 μM concentration, but on the other hand, it was a potent MAGL inhibitor (74 nM). Our data are in accordance with that of Cravatt's group reported for the same compound (JW642).²² On the contrary, the imidazole urea **7g** proved to be potent FAAH inhibitor (17 nM) but very weak MAGL inhibitor. To gain molecular level insights into potency differences of compounds **7f** and **7g** between FAAH and MAGL, molecular docking studies were employed. According to docking both **7f**

and **7g** converged well to the active sites of MAGL and FAAH (Fig. 2), in good accordance with earlier findings.^{14,15,20,23,24} Modeling suggested that in the case of FAAH the bulkiness of the HFIP group can at least partly explain lower FAAH inhibition of compound **7f**. In favorable docking poses, the HFIP moiety is placed in the area of narrow gorge connecting cytosol access and membrane access channels where catalytic serine 241 resides. Due to this carbonyl group of compound **7g** seems to have much easier access to interact with oxyanion hole when compared to carbonyl of **7f**. In the case of MAGL, both compounds fit well to MAGL active site and good convergence is reached. However, placement of HFIP to the polar area of MAGL active site, where glycerol moiety of natural substrate 2-AG forms several hydrogen bond contacts, suggests that higher potency of compound **7f** is at least partly explained by its ability to mimic these interactions (Fig. 2 panel C).^{15,25}

To explore the effect of the position of the distal phenyl ring, we synthesized 4-phenoxy analogs **9a–c**. The 4-phenoxy substituted *p*-nitrophenylcarbamate **9a** showed only modest MAGL and FAAH inhibitory potency, which result is analogous to micromolar MAGL inhibitory potency observed for the 3-phenoxy analog JZL-195.²⁰ The benzotriazole urea **9b** exhibited 9- and 8-fold reduced potency against MAGL and FAAH, respectively, compared to its 3-phenoxy analog **7e**. The imidazole urea **9c** was over 4-fold more potent FAAH inhibitor (3.4 nM) than its 3-phenoxy analog **7g**. In contrast, **9c** displayed only modest MAGL inhibitor potency (660 nM), albeit higher as compared with **7g** (Table 3).

Table 4
MAGL and FAAH inhibitor potencies of methylene-3,4-dioxyphenyl piperidinyl derivatives



Compd	R ₁	R ₂	-logIC ₅₀ (range) [IC ₅₀ nM]	
			hrMAGL ^a	hrFAAH ^b
JJKK-048			9.44 ± 0.05 [0.4] ^c	5.32 ± 0.05 [4800] ^c
11a			7.38 (7.37–7.40) [42]	88 (83–93) ^d
11b			85 (70–101) ^d	89 (85–93) ^d
12a			92 (84–100) ^d	92 (87–96) ^d
12b			89 (85–93) ^d	90 (85–95) ^d
12c			9.16 (9.02–9.30) [0.7]	5.79 (5.69–5.88) [1622]

^a Human recombinant MAGL expressed transiently in HEK293 cells.

^b Human recombinant FAAH expressed transiently in COS7 cells.

^c Ref. 20.

^d Remaining activity at 10 μM (% control (range), *n* = 2).

3.4. Methylene-3,4-dioxyphenyl piperidinyl derivatives

The *p*-nitrophenoxy carbamate JZL184 was originally reported as a highly potent and selective inhibitor of MAGL. However in our assays this compound exhibited much lower MAGL inhibitory activity. Nevertheless, its close triazole urea analog JJKK-048 is highly potent (IC₅₀ 0.2–0.4 nM) and MAGL-selective (>13,000-fold) inhibitor.²⁰ In order to confirm the superior potency of triazole moiety, we synthesized and tested JZL184 analogs (**11a–b** and **12a–c**). As shown in Table 4, the *p*-nitrophenoxy analog **11a** exhibited lower MAGL inhibitory activity (IC₅₀ 42 nM) and its close analog **11b** was not actually able to inhibit MAGL at 10 μM concentration. The FAAH inhibitory activities of both compounds were negligible.

As expected, the triazole urea analog of JZL184 (**12c**) inhibited hrMAGL with high potency (IC₅₀ = 0.7 nM) and displayed notable MAGL selectivity over FAAH (2317-fold), but not reaching the selectivity reported for JJKK-048. Both the replacement of triazole moiety in **12c** with a benzyloxy (**12a**) and 2,2,2-trichloroethoxy (**12b**) abolished the inhibitory potency against FAAH and MAGL, indicating that triazole-moiety is superior leaving group of urea based MAGL inhibitors, while benzyloxy and 2,2,2-trichloroethoxy are poor leaving groups, due to high p*K*_a values of their conjugate acids (~16 and 12, respectively).

4. Conclusion

In this paper, we have demonstrated that the triazole, benzotriazole, and triazolopyridine ureas show activity against MAGL (JJKK-048 and **12c**) whereas the other leaving groups were significantly less active or inactive. As we concluded in our previous paper, triazole heterocycles are good leaving groups because their relatively low conjugate acid p*K*_a values (8–10), that are optimal for

the nucleophilic attack by the MAGL active site catalytic serine. On the other hand, the compounds having the *p*-nitrophenoxy leaving group were effective only in the micromolar-high nanomolar range against MAGL in our assay conditions. The low activity may be due to low p*K*_a of the *p*-nitrophenol (7.15), which makes these compounds excessively reactive so that *p*-nitrophenoxy group is released before reaching the active site of MAGL. In contrast, imidazole (p*K*_a 14.4), benzyloxy (p*K*_a ~ 16), 2,2,2-trichloroethoxy (p*K*_a 12) and arylamines (p*K*_a > 18) are poor leaving groups, and therefore, compounds with these groups were poor MAGL inhibitors. Interesting observation is that *O*-hexafluoroisopropoxy (HFIP) (**7f**) seems to be selective leaving group for MAGL inhibition. The good MAGL inhibition of **7f** can be explained by the optimal p*K*_a of HFIP (9.3) that is close to that of triazole heterocycles, while the low FAAH inhibition potency of **7f** can be explained by the bulkiness of the HFIP moiety, which makes it difficult to access the FAAH active site. In the case of FAAH inhibition, the imidazole moiety seems to be a good leaving group for phenoxyphenyl analogs (**7g** and **9c**), which were approximately 190-fold selective for the inhibition of FAAH. The imidazole urea based FAAH inhibitors have been previously described by Astellas Pharma,²⁶ which asserts the desirable FAAH inhibition of imidazole ureas. The general conclusion is that diverse leaving groups are tolerated for FAAH inhibitors, while MAGL inhibitors should comprise leaving-groups with a conjugate acid p*K*_a of 8–10.

5. Experimental

5.1. General methods

¹H and ¹³C NMR spectra were recorded on a Bruker Avance instrument operating at 500.1 and 25.8 MHz, respectively. Chemical shifts are reported as δ values (ppm) relative to an internal

standard of tetramethylsilane (TMS) or to the solvent line of DMSO ($\delta_{\text{H}} = 2.50$ ppm quintet, $\delta_{\text{C}} = 39.43$ ppm septet). The following abbreviations were used to explain multiplicities: b, broad; d, doublet; m, multiplet; q, quartet; s, singlet; sep, septet; sext, sextet; t, triplet. Electrospray ionization mass spectra were determined on Finnigan MAT LCQ quadrupole ion trap mass spectrometer. Elemental analyses were performed on a ThermoQuest CE instrument (EA 1110 CHNS-O) or a Perkin-Elmer PE 2400 Series II CHNS-O Analyser. The Biotage Initiator 2.0 was used for microwave-assisted synthesis. All chemicals and solvents were of commercial quality and were used without further purification. Most intermediate and end products were purified by flash chromatography using 30–60 μm silica gel and an appropriate eluent

5.1.1. Benzhydrylpiperazin piperazine-1-carbonyl chloride (2)

A solution containing 1-benzhydrylpiperazine **1** (2.13 g, 8.42 mmol) and pyridine (1.6 mL) in anhydrous CH_2Cl_2 was added dropwise to the cooled (-5°C) solution of triphosgene (1.00 g, 3.37 mmol) in anhydrous CH_2Cl_2 . The reaction mixture was slowly warmed up to RT and stirred for 3 h. The reaction was quenched by adding CH_2Cl_2 and water. The organic phase was separated, washed with brine (2×25 mL) and dried with anhydrous Na_2SO_4 . The solvent was evaporated and concentrated in vacuo to yield the crude carbonyl chloride as a yellow solid (2.24 g, yield 84%) which was used for the next step without further purification. ^1H NMR (CDCl_3): δ 7.40 (d, 4H), 7.29 (t, 4H, $J = 7.3$ Hz), 7.21 (t, 2H, $J = 7.3$ Hz), 4.27 (s, 1H), 3.72–3.64 (br s, 4H), 2.44 (s, 4H).

5.1.2. General procedure for synthesis of benzhydrylpiperazinyl carboxamides and from benzhydrylpiperazin piperazine-1-carbonyl chloride

In the suspension of piperazine-1-carbonyl chloride (**2**) (1.1 equiv), aniline/heterocyclic amine (1.0 equiv) and DMAP (0.1 equiv) in anhydrous THF was added diisopropylethylamine (DIPEA) (1.6 equiv) via a syringe under argon. Reaction mixture was stirred overnight at room temperature (RT). The reaction was quenched by adding EtOAc and water into the reaction mixture. The organic layer was washed with brine, dried over sodium sulfate and evaporated. The crude product was chromatographed in a silica gel column using a gradient solvent system of PE/EtOAc (1:0–0:1) to obtain the final compound.

Compounds JJKK-048, AKU-002, AKU-003, AKU-015, AKU-005, AKU-009, AKU-010, AKU-033, AKU-034, SAR629 (JJKK-033), and JJKK-006 were prepared and characterized as previously reported.²⁰

5.1.3. 4-Benzhydryl-N-phenylpiperazine-1-carboxamide (3a)

Compound **3a** was obtained from 4-benzhydrylpiperazine-1-carbonyl chloride (**2**) (0.35 g, 1.11 mmol), DMAP (6 mg, 0.05 mmol), aniline (0.09 mL, 1.01 mmol) and diisopropylethylamine (DIPEA) (0.30 mL, 1.76 mmol). The crude product (0.35 g) was purified on a silica gel column as described in general procedure to give **3a** as a white solid (0.15 g, 39%). ^1H NMR (CDCl_3): δ 7.42 (d, 4H, $J = 7.3$ Hz), 7.34–7.27 (m, 8H), 7.20 (t, 2H, $J = 7.3$ Hz), 7.01 (t, 1H, $J = 7.3$ Hz), 6.26 (s, 1H), 4.27 (s, 1H), 3.50–3.48 (m, 4H), 2.46–2.44 (m, 4H). ESI-MS (m/z) 372.18 (M⁺). Anal. Calcd for $\text{C}_{24}\text{H}_{25}\text{N}_3\text{O} \times 0.1\text{H}_2\text{O}$: C 77.60, H 6.78, N 11.36. Found: C 76.99, H 7.10, N 11.01.

5.1.4. 4-Benzhydryl-N-(4-(trifluoromethyl)phenyl)piperazine-1-carboxamide (3b)

Compound **3b** was obtained from 4-benzhydrylpiperazine-1-carbonyl chloride (**2**) (0.40 g, 1.27 mmol), 4-(trifluoromethyl)aniline (0.09 g, 0.58 mmol), DMAP (4 mg, 0.03 mmol) and DIPEA (0.20 mL, 0.86 mmol). The crude product (0.41 g) was purified on a silica gel column (12 g) as described in general procedure to give **3b** as a white solid (40 mg, 19%). ^1H NMR (CDCl_3): δ 7.52 (d, 2H,

$J = 7.9$ Hz), 7.46 (d, 2H, $J = 8.4$ Hz), 7.42 (d, 4H, $J = 7.9$ Hz), 7.30 (t, 4H, $J = 7.5$ Hz), 7.21 (t, 2H, $J = 7.1$ Hz), 6.42 (s, 1H), 4.28 (s, 1H), 3.52–3.50 (m, 4H), 2.47–2.45 (m, 4H). ESI-MS (m/z) 440.07 (M⁺). Anal. Calcd for $\text{C}_{25}\text{H}_{24}\text{N}_3\text{O}\text{F}_3$: C 68.32, H 5.50, N 9.56. Found: C 68.15, H 5.80, N 9.46.

5.1.5. 4-Benzhydryl-N-(4-nitrophenyl)piperazine-1-carboxamide (3c)

Compound **3c** was obtained from **2** (0.40 g, 1.27 mmol), 4-nitroaniline (0.08 g, 0.58 mmol), DMAP (4 mg, 0.03 mmol) and DIPEA (0.20 mL, 0.86 mmol). The crude product (0.41 g) was purified on a silica gel column as described in general procedure to give **3c** as a yellow solid (0.19 g, 77%). ^1H NMR (CDCl_3): δ 8.07 (d, 2H, $J = 9.0$ Hz), 7.39–7.37 (m, 4H), 7.28–7.24 (m, 4H, $J = 7.3$ Hz), 7.20–7.15 (m, 2H), 6.62 (d, 2H, $J = 9.0$ Hz), 4.34 (br s, 2H), 3.57–3.19 (m, 4H), 3.45–3.27 (m, 4H), ^{13}C NMR (CDCl_3): δ 152.4, 149.7, 142.1, 128.64, 127.84, 127.20, 126.35, 113.39, 75.86, 51.52, 51.20, 46.92, 45.34 and 44.35. ESI-MS (m/z) only a fragment 167.05 ($\text{C}_{13}\text{H}_{11}^+$) was identified. Anal. Calcd for $\text{C}_{24}\text{H}_{24}\text{N}_4\text{O}_3 \times 1.2\text{H}_2\text{O}$: C 69.21, H 5.81, N 13.45. Found: C 65.49, H 6.31, N 13.19.

5.1.6. 4-Benzhydryl-N-(4-butylphenyl)piperazine-1-carboxamide (3d)

Compound **3d** was obtained from **2** (0.36 g, 1.14 mmol), 4-butylaniline (0.08 g, 0.57 mmol), DMAP (3 mg, 0.03 mmol) and DIPEA (0.15 mL, 0.78 mmol). The crude product (0.37 g) was purified on a silica gel column (12 g) as described in general procedure to give **3d** as a white solid (30 g, 14%). ^1H NMR (CDCl_3): δ 7.43–7.41 (m, 4H), 7.28 (t, 4H, $J = 7.4$ Hz), 7.21 (t, 4H, $J = 7.5$ Hz), 7.08 (d, 2H, $J = 8.1$ Hz), 6.19 (s, 1H), 4.26 (s, 1H), 3.48, (m, 4H), 2.54, (t, 2H, $J = 7.7$ Hz), 2.44 (m, 4H), 1.55, (qui, 2H, $J = 7.7$ Hz), 1.33 (sext, 2H, $J = 7.5$ Hz), 0.90 (t, 3H, $J = 7.4$ Hz). ESI-MS (m/z) 428 (MH⁺). Anal. Calcd for $\text{C}_{28}\text{H}_{33}\text{N}_3\text{O}$: C 78.65, H 7.78, N 9.83. Found C 78.45, H 8.16, N 9.90.

5.1.7. 4-Benzhydryl-N-(4-methoxyphenyl)piperazine-1-carboxamide (3e)

Compound **3e** was obtained from **2** (0.40 g, 1.27 mmol), *p*-anisidine (0.08 g, 0.58 mmol), DMAP (**5**) (4 mg, 0.03 mmol) and DIPEA (0.15 mL, 0.86 mmol). Reaction mixture was stirred over two nights at room temperature. The crude product (0.37 g) was purified on a silica gel column as described in general procedure to give **3e** as a white solid (0.22 g, 93%). ^1H NMR (CDCl_3): δ 7.42 (br d, 4H, $J = 7.3$ Hz), 7.29 (t, 4H, $J = 7.6$ Hz), 7.22 (d, 2H, $J = 8.9$ Hz), 7.20 (t, 2H, $J = 7.4$ Hz), 6.82 (d, 2H, $J = 8.9$ Hz), 6.14 (s, 1H), 4.26 (s, 1H), 3.77 (s, 3H), 3.48–3.46 (m, 4H), 2.45–2.43 (m, 4H). ESI-MS (m/z) 402.14 (M⁺). Anal. Calcd for $\text{C}_{25}\text{H}_{27}\text{N}_3\text{O}_2 \times 0.15\text{H}_2\text{O}$: C 74.79, H 6.78, N 10.47, Found C 74.61, H 7.22, N 10.21.

5.1.8. (4-Benzhydrylpiperazin-1-yl)(4-phenyl-1H-imidazol-1-yl) methanone (3f)

Compound **3f** was obtained from **2** (0.32 g, 1.02 mmol), 4-phenyl-1H-imidazole (0.17 g, 1.02 mmol), DMAP (10 mg, 0.05 mmol) and DIPEA (0.40 mL, 2.34 mmol). The crude product (0.46 g) was purified on a silica gel column as described in general procedure to give **3f** as a white solid (0.31 g, yield 71%). ^1H NMR (CDCl_3): δ 7.88 (s, 1H), 7.76 (d, 2H, $J = 7.4$), 7.43–7.41 (dt, 5H, $J = 7.4$ Hz, $J = 2.3$ Hz), 7.38 (t, 2H, $J = 7.8$ Hz), 7.30 (t, 5H, $J = 7.5$ Hz), 7.21 (t, 2H, $J = 7.3$ Hz), 4.31 (s, 1H), 3.67 (s, 4H), 2.50 (s, 4H). ESI-MS (m/z) 423.21 (M⁺). Anal. Calcd for $\text{C}_{27}\text{H}_{26}\text{N}_4\text{O} \times 0.4\text{H}_2\text{O}$: C 75.46, H 6.29, N 13.04. Found: C 75.65, H 6.31, N 13.29.

5.1.9. Phenyl pyridin-2-yl-carbamate (5a)

To a solution of 2-aminopyridine (0.20 g, 2.13 mmol) in anhydrous MeCN cooled to 0°C in ice bath was added dropwise mixture of phenyl chloroformate (**4a**) (0.25 mL, 2.34 mmol), Et_3N (0.22 mL,

2.13 mmol) and DMAP (30 mg, 0.21 mmol) in anhydrous MeCN. Reaction mixture was allowed to warm at RT and was kept stirring overnight. Reaction was diluted with 60 mL of EtOAc and organic phase was washed successively with 0.5 M HCl (3 × 25 mL), 1 N NaOH (2 × 25 mL), brine (2 × 25 mL) and water (2 × 25 mL). The organic phase was dried over Na₂SO₄, evaporated and concentrated in vacuo. The crude intermediate (0.30 g) was purified on a silica gel column eluting with a gradient of EtOAc/petroleum ether to give **5a** as a white solid (0.23 g, 50%). ¹H NMR (DMSO-*d*₆): δ 8.61 (br d, 1H, *J* = 3.5 Hz), 8.04 (td, 1H, *J* = 7.7, 1.9 Hz), 7.91 (br d, 1H, *J* = 8.0 Hz), 7.51 (ddd, 1H, *J* = 7.4, 4.8, 0.9 Hz), 7.44 (t, 4H, *J* = 7.9 Hz), 7.31 (t, 1H, *J* = 7.4 Hz), 7.20 (d, 2H, *J* = 7.6 Hz).

5.1.10. 4-Nitrophenyl pyridin-3-ylcarbamate (**5b**)

To a solution of 3-aminopyridine (0.20 g, 2.13 mmol) in anhydrous MeCN cooled to 0 °C in ice bath was added dropwise mixture of 4-nitrophenyl chloroformate (**4b**) (0.47 g, 2.34 mmol), Et₃N (0.24 mL, 2.34 mmol) and DMAP (30 mg, 0.21 mmol) in anhydrous MeCN, keeping the reaction mixture on ice. Reaction mixture was allowed to warm at RT and was kept stirring for 5 h. Then it was diluted with EtOAc, washed with 0.5 M HCl, 1 N NaOH, brine and H₂O, dried over Na₂SO₄, and concentrated in vacuo, to obtain **5a** as a white solid (0.30 g, yield 55%). ¹H NMR (CD₃OD): δ 8.60 (s, 1H), 8.18 (dd, 1H, *J* = 4.8, 1.3 Hz), 8.12 (AA'BB' system, 2H, *J* = 9.2 Hz), 7.99 (d, 1H, *J* = 8.4 Hz), 7.36 (ddd, 1H, *J* = 8.4, 4.8, 0.6 Hz), 6.88 (AA'BB' system, 2H, *J* = 9.2 Hz).

5.1.11. 4-Benzhydryl-*N*-(pyridin-3-yl)piperazine-1-carboxamide (**3g**)

To a solution of 4-nitrophenyl pyridin-3-ylcarbamate (**5b**) (0.30 g, 1.17 mmol) in anhydrous MeCN (20 mL) was added mixture of 1-benzhydrylpiperazine (**1**) (0.19 g, 0.64 mmol), pyridine (0.10 mL, 1.17 mmol) in anhydrous MeCN (10 mL) dropwise. Reaction mixture was refluxed for 2.5 h and cooled down to RT. The reaction mixture was concentrated in vacuo and residue was purified by flash chromatography on silica gel column eluting with a gradient of EtOAc/petroleum ether to give **3g** as a white solid (0.28 g, yield 98%). ¹H NMR (CD₃OD): δ 8.56 (d, 1H, *J* = 2.3 Hz), 8.15 (dd, 1H, *J* = 4.7, 1.3 Hz), 7.89 (ddd, 1H, *J* = 8.4, 2.3, 1.3 Hz), 7.46 (d, 4H, *J* = 7.3 Hz), 7.33 (ddd, 1H, *J* = 8.4, 4.7, 0.6 Hz), 7.29 (t, 4H, *J* = 7.6 Hz), 7.19 (t, 2H, *J* = 7.4 Hz), 4.30 (s, 1H), 3.56 (m, 4H), 2.45 (m, 4H). ESI-MS (*m/z*) 373.15 (M⁺). Anal. Calcd for C₂₃H₂₄N₄O: C 74.17, H 6.49, N 15.04. Found: C 73.87, H 6.89, N 14.97.

5.1.12. 4-Benzhydryl-*N*-(pyridin-2-yl)piperazine-1-carboxamide (**3h**)

A mixture of phenyl pyridin-2-yl-carbamate (**5a**) (0.18 g, 0.82 mmol), 1-benzhydrylpiperazine (**1**) (0.21 g, 0.82 mmol), and pyridine (0.07 mL, 0.82 mmol) in anhydrous MeCN (4 mL) was placed in the microwave reactor and heated to 120 °C for 15 min. The reaction mixture was concentrated in vacuo, and the crude product was purified on a silica gel column to give **3h** as a white solid (50 mg, 13%). ¹H NMR (MeOD): δ 8.19 (d, 1H, *J* = 4.9 Hz), 7.75 (d, 1H, *J* = 8.4 Hz), 7.69 (ddd, 1H, *J* = 8.4, 6.9, 1.7 Hz), 7.46 (d, 4H, *J* = 7.3 Hz), 7.29 (t, 4H, *J* = 7.6 Hz), 7.19 (t, 2H, *J* = 7.4 Hz), 7.00 (ddd, 1H, *J* = 6.9, 4.9, 1.1 Hz), 4.29 (s, 1H), 3.57 (m, 4H), 2.45 (m, 4H). ESI-MS (*m/z*) 373.18 (M⁺). Anal. Calcd for C₂₃H₂₄N₄O × 0.1H₂O: C 74.17, H 6.49, N 15.04. Found: C 73.43, H 6.79, N 14.74.

5.1.13. 4-(3-Phenoxybenzyl)-*N*-phenylpiperazine-1-carboxamide (**7a**)

1-(3-Phenoxybenzyl)-piperazine (**6**)²⁰ (150 mg, 0.559 mmol) and pyridine (110 μL, 1.49 mmol) were dissolved in CH₂Cl₂ and triphosgene (95 mg, 0.32 mmol) was added in three equal portions.

The mixture was kept at 0 °C for 30 min, after which the temperature was allowed to reach RT. After 3 h the mixture was concentrated in vacuo, and the crude carbonyl chloride was used in the next step without further purification. The reaction mixture of crude carbonyl chloride, DIPEA (211 μL, 2.1 equiv), DMAP (7.5 mg, 0.1 equiv), and aniline (51 μL, 0.56 mmol) in anhydrous THF (4 mL) was stirred on ice at 0 °C for 30 min and then allowed to warm to RT and stirring was continued for 60 h. The mixture was concentrated in vacuo and the residue was purified by silica gel column chromatography eluting with a gradient of EtOAc–MeOH (from 1:0 to 0.99:0.01) to give **7a** (105 mg, 48%). ¹H NMR (500 MHz, CDCl₃) δ 2.48 (m, 4H), 3.49 (s, 2H), 3.92 (br s, 4H), 6.29 (br s, 1H), 6.91 (dd, *J* = 8.1, 2.4 Hz, 1H), 6.99–7.06 (m, 3H), 7.07 (d, *J* = 7.7 Hz, 1H), 7.11 (t, *J* = 7.4 Hz, 1H), 7.26–7.36 (m, 8H). ESI-MS (*m/z*) 488.06 (MH⁺). Anal. Calcd for C₂₄H₂₅N₃O₂: C 74.39, H 6.50, N 10.84. Found: C 73.91, H 6.60, N 10.86.

5.1.14. 4-(3-Phenoxybenzyl)-*N*-(4-nitrophenyl)piperazine-1-carboxamide (**7b**)

To a mixture of **6** (53 mg, 0.20 mol) in THF was added 4-nitrophenyl isocyanate (29 mg, 0.18 mmol) and the mixture was refluxed at 80 °C for overnight. The mixture was concentrated in vacuo and residue was purified by silica gel column chromatography with gradient of EtOAc–MeOH (from 1:0 to 0.975:0.025) to give 49 mg (57%) of **7b**. ¹H NMR (500 MHz, CDCl₃) δ 2.51 (m, 4H), 3.53 (m, 4H), 3.54 (s, 2H), 6.67 (br s, 1H), 6.91 (dd, *J* = 8.0, 2.4 Hz, 1H), 6.99–7.04 (m, 3H), 7.06 (d, *J* = 7.7 Hz, 1H), 7.11 (tt, *J* = 7.5, 1.1 Hz, 1H), 7.29 (t, *J* = 7.9 Hz, 1H), 7.34 (dd, *J* = 8.7, 7.4 Hz, 2H), 7.52 (d, *J* = 9.1 Hz, 2H), 8.17 (d, *J* = 9.2 Hz, 2H). ESI-MS (*m/z*) 433.15 (MH⁺). Anal. Calcd for C₂₄H₂₄N₄O₄: C 66.56, H 5.59, N 12.95. Found: C 66.02, H 5.59, N 13.00.

5.1.15. 4-(3-Phenoxybenzyl)-*N*-(4-methoxyphenyl)piperazine-1-carboxamide (**7c**)

To a mixture of **6** (54 mg, 0.20 mol) in THF was added 4-methoxyphenyl isocyanate (30 mg, 0.20 mmol) and the mixture was refluxed at 80 °C for overnight. The mixture was concentrated in vacuo and residue was purified by silica gel column chromatography with gradient of EtOAc–MeOH (from 1:0 to 0.995:0.005) to give 67 mg (80%) of **7c**. ¹H NMR (500 MHz, CDCl₃) δ 2.48 (m, 4H), 3.47 (m, 4H), 3.52 (s, 2H), 3.77 (s, 3H), 6.18 (br s, 1H), 6.83 (d, *J* = 9.1 Hz, 2H), 7.90 (dd, *J* = 8.1, 2.9 Hz, 1H), 6.99–7.04 (m, 3H), 7.07 (d, *J* = 7.6 Hz, 1H), 7.11 (t, *J* = 7.4 Hz, 1H), 7.23 (d, *J* = 9.1 Hz, 2H), 7.28 (t, *J* = 7.8 Hz, 1H), 7.34 (dd, *J* = 8.6, 7.4 Hz, 2H). ESI-MS (*m/z*) 418.04 (MH⁺). Anal. Calcd for C₂₅H₂₇N₃O₃ × 0.1H₂O: C 71.61, H 6.54, N 10.02. Found: C 71.20, H 6.74, N 9.75.

5.1.16. (1*H*-Benzo[*d*][1,2,3]triazol-1-yl)(4-(3-phenoxybenzyl)-piperazin-1-yl)-methanone (**7d**)

A solution of **6** (185 mg, 0.559 mmol), 1*H*-benzo[*d*][1,2,3]triazole (44.6 mg, 0.375 mmol), DMAP (3.0 mg, 0.025 mmol) and DIPEA (0.13 mL, 0.761 mmol) in anhydrous THF (6 mL) was stirred overnight at RT. The reaction mixture was diluted by addition of EtOAc (25 mL) and water (13 mL). The organic phase was washed twice with saturated NaCl solution and dried over Na₂SO₄. The solvents were evaporated to dryness and the residue was purified by column chromatography on silica gel eluting with a gradient of EtOAc/CH₂Cl₂ to afford **7d** as a light yellow solid (55 mg, 35%). ¹H NMR (500 MHz, CDCl₃) δ 2.63 (br s, 4H), 3.57 (s, 2H), 3.92 (br s, 4H), 6.91 (dd, *J* = 8.4, 2.1 Hz, 1H), 6.99–7.06 (m, 3H), 7.08 (d, *J* = 7.9 Hz, 1H), 7.11 (t, *J* = 7.4 Hz, 1H), 7.29 (t, *J* = 7.9 Hz, 1H), 7.34 (dd, *J* = 8.6, 7.4 Hz, 2H), 7.45 (td, *J* = 7.7, 1.1 Hz, 1H), 7.60 (td, *J* = 7.7, 1.0 Hz, 1H), 7.99 (d, *J* = 8.4 Hz, 1H), 8.09 (d, *J* = 8.4 Hz, 1H). ESI-MS (*m/z*) 414.1 (M⁺). Anal. Calcd for C₂₄H₂₃N₅O₂: C 67.81, H 5.60, N 16.37. Found: C 69.72, H 5.61, N 16.94.

5.1.17. (3H-[1,2,3]Triazol[4,5-b]pyridin-3-yl)(4-(3-phenoxybenzyl)-piperazin-1-yl)methanone (7e)

A solution of **6** (300 mg, 0.907 mmol), 1H-[1,2,3]-triazolo[4,5-b]pyridine (73 mg, 0.608 mmol), DMAP (4.87 mg, 0.040 mmol), and DIPEA (0.211 mL, 1.233 mmol) in anhydrous THF (7.7 mL) was stirred overnight at RT. The reaction was diluted by addition of EtOAc (23 mL) and water (12 mL). The organic phase was washed twice with saturated NaCl solution, and dried over Na₂SO₄. The solvents were evaporated to dryness and the residue was purified by column chromatography on silica gel eluting with a gradient of EtOAc/petroleum ether to give waxy solid (125 mg, yield 33%). ¹H NMR (500 MHz, CDCl₃): δ 2.65 (t, *J* = 5.0 Hz, 4H), 3.58 (s, 2H), 3.90 (br s, 2H), 4.03 (br s, 2H), 6.92 (dd, *J* = 7.7, 2.0 Hz, 1H), 7.00–7.06 (m, 3H), 7.08 (d, *J* = 7.6 Hz, 1H), 7.11 (t, *J* = 7.4 Hz, 1H), 7.30 (t, *J* = 7.9 Hz, 1H), 7.35 (t, *J* = 8.4 Hz, 2H), 7.6 (dd, *J* = 8.2, 4.4 Hz, 1H), 8.38 (dd, *J* = 8.5, 1.6 Hz, 1H), 8.81 (dd, *J* = 4.4, 1.6 Hz, 1H). ESI-MS (*m/z*) 414.8 (M⁺). Anal. Calcd for C₂₃H₂₃N₆O₂: C 66.65, H 5.35, N 20.28. Found: C 65.65, H 5.39, N 18.94.

5.1.18. 1,1,1,3,3,3-Hexafluoropropan-2-yl 4-(3-phenoxybenzyl)piperazine-1-carboxylate (7f, JW642)

To a stirring mixture of hexafluoroisopropanol (80 μL, 0.760 mmol), DIPEA (260 μL, 1.49 mmol) in CH₂Cl₂ (4 mL) was added triphosgene (66 mg, 0.220 mmol) at 0 °C. After stirring for 30 min at 0 °C the mixture was allowed to warm up to RT and stirred for 2 h. Compound **6** (191 mg, 0.712 mmol) dissolved in 4 mL of CH₂Cl₂ was added to the mixture at 0 °C and stirred overnight. Solvents were concentrated in vacuo and the residue was purified by silica gel column chromatography eluting with a gradient of hexane–EtOAc (from 99:1 to 85:15) to give **7f** as syrup (97 mg, 28%). ¹H NMR (500 MHz, CDCl₃) δ 2.44 (m, 4H), 3.51 (s, 2H), 3.54 (m, 4H), 5.74 (sep, *J* = 6.3 Hz, 1H) 6.90 (ddd, *J* = 8.2, 2.7, 0.9 Hz, 1H), 6.98–7.02 (m, 3H), 7.04 (d, *J* = 7.6 Hz, 1H), 7.10 (tt, *J* = 7.4, 1.1 Hz, 1H), 7.85 (d, *J* = 7.9 Hz, 1H), 7.34 (dd, *J* = 8.6, 7.4 Hz, 2H). ESI-MS (*m/z*) 462.19 (M⁺). Anal. Calcd for C₂₁H₂₀F₆N₂O₃: C 54.55, H 4.36, N 6.06. Found: C 55.08, H 4.10, N 6.02.

5.1.19. (1H-Imidazol-1-yl)(4-(3-phenoxybenzyl)piperazin-1-yl)methanone (7g)

To a solution of **6** (150 mg, 0.555 mmol), DIPEA (190 μL, 1.1 mmol) in THF (4 mL) at 0 °C was added dropwise 1,1'-carbonyldiimidazole (CDI, 1 equiv, 85 mg, 0.555 mmol) over 10 min. After addition the mixture was allowed to warm up to RT and stirred overnight. The organic layer was washed with water, dried over anhydrous MgSO₄, and concentrated in vacuo. The residue was purified by silica gel column chromatography eluting with a gradient of EtOAc–MeOH (from 99:1 to 90:10) to give **7g** as oily substance (94 mg, 47%). ¹H NMR (500 MHz, CDCl₃) δ 2.52 (m, 4H), 3.53 (s, 2H), 3.61 (m, 4H), 6.91 (ddd, *J* = 8.1, 2.5, 1.0 Hz, 1H), 6.98–7.02 (m, 3H), 7.04 (d, *J* = 7.6 Hz, 1H), 7.09 (dd, *J* = 1.5, 1.1 Hz, 1H), 7.29 (tt, *J* = 7.3, 1.1 Hz, 1H), 7.18 (t, *J* = 1.4 Hz, 1H), 7.28 (t, *J* = 7.8 Hz, 1H), 7.34 (dd, *J* = 8.6, 7.4 Hz, 2H), 7.86 (dd, *J* = 1.2, 1.0 Hz, 1H). ESI-MS (*m/z*) 463.16 (MH⁺). Anal. Calcd for C₂₁H₂₂N₄O₂: C 69.59, H 6.12, N 15.46. Found: C 69.01, H 6.15, N 15.54.

5.1.20. 4-Nitrophenyl-4-(4-phenoxy-benzyl)-piperazine-1-carboxylate (9a)

To a solution of 1-(4-phenoxybenzyl)-piperazine (**8**)²⁰ (350 mg, 1.304 mmol) in anhydrous CH₂Cl₂ (2.7 mL) was added DIPEA (1.75 mL, 10.0 mmol) and 4-nitrophenyl chloroformate (342 mg, 1.70 mmol), and solution was stirred at RT for 15 h. The reaction was quenched with 2 M NaOH (2 mL) and the layers separated. The aqueous layer was extracted with EtOAc and the combined organics were washed with 2 M NaOH (3×) and brine, and dried over Na₂SO₄. The solvents were evaporated to dryness, and residue was purified by flash chromatography on silica gel, eluting first

with a gradient of EtOAc/hexane, to give slightly yellow solid (442 mg, yield 78%). ¹H NMR (500 MHz, CDCl₃): δ 2.52 (t, *J* = 1.0 Hz, 4H), 3.54 (s, 2H), 3.60 (br s, 2H), 3.69 (br s, 2H), 6.98 (d, *J* = 8.2 Hz, 2H), 7.02 (d, *J* = 8.2 Hz, 2H), 7.11 (t, *J* = 7.60 Hz, 1H), 7.29 (m, 4H), 7.34 (t, *J* = 7.9 Hz, 2H), 8.25 (d, *J* = 8.8 Hz, 2H). ESI-MS (*m/z*) 434.0 (M⁺). Anal. Calcd for C₂₄H₂₃N₃O₅: C 66.50, H 5.35, N 9.69. Found: C 65.99, H 5.37, N 9.48.

5.1.21. (1H-Benzo[d][1,2,3]triazol-1-yl)(4-(4-phenoxybenzyl)-piperazin-1-yl)methanone hydrochloride (9b)

To a solution of bis(1H-benzo[d][1,2,3]triazol-1-yl)methanone²¹ (240 mg, 0.908 mmol) in THF (20 mL) was added **8** (350 mg, 1.304 mmol) and the mixture was heated in a microwave oven (130 °C) for 2.5 h. The reaction mixture was evaporated to dryness and the residue was chromatographed over a silica gel column using gradient solvent system of MeOH–CH₂Cl₂ (2:98–0:100) to give free amine of **9b** as an oil. It was converted to its HCl salt by dissolving it in EtOAc and adding dropwise solution of 2.5 M HCl in EtOAc until the solution was acidic. Excess of HCl was removed by bubbling with nitrogen gas. EtOAc was evaporated, and the precipitated product was washed three times with hexane to afford **9b** hydrochloride as a white crystalline solid (162 mg, 43%). ¹H NMR (500 MHz, CDCl₃): δ 2.64 (br s, 4H), 3.57 (s, 2H), 3.94 (br s, 4H), 6.98 (d, *J* = 8.5 Hz, 2H), 7.00–7.05 (m, 2H), 7.10 (t, *J* = 7.6 Hz, 1H), 7.30 (d, *J* = 8.5 Hz, 2H), 7.34 (td, *J* = 8.5, 0.9 Hz, 2H), 7.45 (td, *J* = 7.9, 0.8 Hz, 1H), 7.60 (td, *J* = 8.2, 0.9 Hz, 1H), 7.99 (d, *J* = 7.9 Hz, 1H), 8.09 (d, *J* = 8.2 Hz, 1H). ESI-MS (*m/z*) 414.1 (M⁺). Anal. Calcd for C₂₃H₂₄ClN₅O₂: C 64.07, H 5.38, N 15.57. Found: C 64.25, H 5.38, N 15.78.

5.1.22. (1H-imidazol-1-yl)(4-(4-phenoxy-benzyl)-piperazin-1-yl)-methanone hydrochloride 9c

A mixture of **8** (300 mg, 1.12 mmol) and 1,1'-carbonyldiimidazole (CDI, 199 μL, 1.23 mmol) in THF (15 mL) was heated first 1 h at 80 °C, then 1 h at 90 °C, and 1 h at 110 °C under microwave irradiation. Since the reaction was not completed, additional CDI (100 mg, 6.17 mmol) was added and microwave heating was continued for 1 h at 120 °C. The reaction mixture was evaporated to dryness and the residue was purified by silica gel column chromatography eluting with a gradient of MeOH–CH₂Cl₂ (from 99:1 to 90:10) to give **9c** as oily substance which was converted to its HCl salt as described for **9b**. The precipitated product was washed three times with hexane to afford **9b** hydrochloride as a white crystalline solid (39 mg, 9%). ¹H NMR (500 MHz, CD₃OD): δ 3.36 (br s, 4H), 3.91 (br s, 4H), 4.33 (s, 2H), 7.01–7.09 (m, 4H) 7.16–7.22 (m, 2H), 7.40 (td, *J* = 7.3, 1.0 Hz, 2H), 7.51–7.59 (m, 3H), 8.30 (s, 1H). ESI-MS (*m/z*) 363.1 (M⁺). Anal. Calcd for C₂₁H₂₃ClN₄O₂ × 0.4H₂O: C 62.11, H 5.91, N 13.80. Found: C 61.79, H 5.79, N 13.40.

5.1.23. 1-Benzyl 4-ethyl piperidine-1,4-dicarboxylate (14)

Benzyl chloroformate (11.9 g, 70.0 mmol) was added dropwise to a solution of ethyl isonipecotate (**13**) (10.0 g, 63.6 mmol) and Et₃N (11.5 mL, 83.0 mmol) in CHCl₃ (140 mL) at 0 °C. After addition, the reaction mixture was stirred at 0 °C for 1 h, then allowed to warm up to room temperature and stirred overnight. The reaction mixture was washed brine, with 2 M HCl, and again with brine. The solution was dried over magnesium sulfate and concentrated in vacuo. The residue (6.10 g, 66% yield) was used without further purification. ¹H NMR (CDCl₃, 500 MHz): δ 1.26 (3H, t, *J* = 7.1 Hz), 1.66 (2H, dq, *J* = 11.6, 3.4 Hz), 1.84–1.95 (2H, m), 2.46 (1H, tt, *J* = 11.0, 4.0 Hz), 2.93 (2H, t, *J* = 10.4 Hz), 4.14 (2H, q, *J* = 7.1 Hz), 4.02–4.17 (2H, m), 5.13 (2H, s), 7.28–7.39 (5H, m).

5.1.24. 4-Nitrophenyl-4-(bis(benzo[d][1,3]dioxol-5-yl)methyl)piperidine-1-carboxylate (11a)

To a solution of **10a**²⁰ (250 mg, 0.737 mmol) in anhydrous CH₂Cl₂ (20 mL) was added Et₃N (0.534 mL, 3.83 mmol) and

4-nitrophenyl chloroformate (233 mg, 1.16 mmol), and solution was stirred at RT for 15 h. The mixture was diluted with CH₂Cl₂, washed with satd Na₂CO₃ solution and brine, and dried over Na₂SO₄. The solvents were evaporated to dryness, and residue was purified twice by flash chromatography on silica gel, eluting first with a gradient of EtOAc/petroleum ether and followed with a gradient of MeOH/CH₂Cl₂, to give yellow solid (89 mg, yield 24%). ¹H NMR (500 MHz, CDCl₃): δ 1.18 (q, *J* = 12.3 Hz, 2H), 1.69 (d, *J* = 12.9 Hz, 2H), 2.10–2.23 (m, 1H), 2.84 (t, *J* = 12.3 Hz, 1H), 2.98 (t, *J* = 12.3 Hz, 1H), 3.37 (d, *J* = 10.7 Hz, 1H), 4.22 (t, *J* = 13.9 Hz, 2H), 5.92 (dd, *J* = 6.15, 1.1 Hz, 4H), 6.65–6.81 (m, 6H), 7.27 (d, *J* = 9.1 Hz, 2H), 8.24 (d, *J* = 9.1 Hz, 2H). ESI-MS (*m/z*) 504.9 (M⁺). Anal. Calcd for C₂₇H₂₄N₅O₈: C 64.28, H 4.80, N 5.55. Found: C 63.03, H 4.78, N 5.33.

5.1.25. 4-Nitrophenyl-4-[bis(benzo[d][1,3]dioxo-5-yl)methylene]-piperidine-1-carboxylate (11b)

To a solution of **10b**²⁰ (320 mg 0.949 mmol) in anhydrous CH₂Cl₂ (20 mL) was added Et₃N (0.688 mL, 4.93 mmol) and 4-nitrophenyl chloroformate (285 mg, 1.414 mmol), and solution was stirred at RT for 15 h. The mixture was diluted with CH₂Cl₂, washed with Na₂CO₃ solution and brine, and dried over Na₂SO₄. The solvents were evaporated on a rotary evaporator and the vac. and residue was purified twice by flash chromatography on silica gel, eluting with a gradient of EtOAc/petroleum ether, to give a light brown solid (300 mg, yield 63%). ¹H NMR (500 MHz, CD₃OD): δ 2.46 (br s, 4H), 3.60 (br s, 2H), 3.68 (br s, 2H), 5.94 (s, 4H), 6.55–6.63 (m, 4H), 6.76 (d, *J* = 7.9 Hz, 2H), 7.30 (d, *J* = 9.1 Hz, 2H), 8.25 (d, *J* = 9.1 Hz, 2H). ESI-MS (*m/z*) 503.0 (M⁺). Anal. Calcd for C₂₇H₂₂N₅O₈: C 64.54, H 4.41, N 5.58. Found: C 63.83, H 4.61, N 5.29.

5.1.26. Benzyl 4-(dibenzo[d][1,3]dioxol-5-yl)(hydroxy)methyl-piperidine-1-carboxylate (12a)

Compound **12a** was prepared according to previous procedure,²⁷ using 4-bromo-1,2-methylenedioxybenzene (4.02 g, 20 mmol), *n*-BuLi (12.5 mL, 1.6 M in toluene, 20 mmol) and **14** (2.04 g, 7.00 mmol). Purification of the crude oil by flash chromatography on silica gel gave **12a** (815 mg, 24% yield). ¹H NMR (CDCl₃, 500 MHz): δ 1.30 (qd, *J* = 3.9, 12.6 Hz, 2H), 1.55 (br s, 2H), 2.39 (tt, *J* = 2.9, 11.8 Hz, 1H), 2.77 (br t, *J* = 10.8 Hz, 2H), 4.23 (br s, 2H), 5.10 (s, 2H), 5.92 (s, 4H), 6.73 (d, *J* = 7.9 Hz, 2H), 6.88–6.92 (m, 4H), 7.24–7.33 (m, 5H).

5.1.27. (4-(Bis(benzo[d][1,3]dioxol-5-yl)(hydroxy)methyl)-piperidin-1-yl)(1*H*-1,2,4-triazol-1-yl)methanone (12c)

Compound **12a** (775 mg, 1.58 mmol) was hydrogenated as previously described²⁷ to yield 560 mg (100%) of bis(benzo[d][1,3]dioxol-5-yl)(piperidin-4-yl)methanol (**15**). ¹H NMR (CDCl₃/DMSO-*d*₆, 500 MHz): δ 1.63 (m, 2H), 1.74 (m, 2H), 2.88 (m, 2H), 3.59 (m, 2H), 3.92 (br s, 1H), 5.10 (br s, 1H), 5.91 (s, 4H), 6.72 (d, *J* = 7.9 Hz, 2H), 6.95 (d, *J* = 7.9 Hz, 2H), 6.97 (s, 2H). Portion of the resulting alcohol (100 mg, 0.28 mmol) was dissolved in THF (5 mL) and 1,1'-carbonyl-di-(1,2,4-triazole) (CDT) was added as one portion, followed by DIPEA. After stirring for several days, reaction was not completed. Additional portion (40 mg) of CDT was added with DMF (5 mL) and stirred for 6 h after which solution turned clear. Solvents were evaporated. CH₂Cl₂ was added and solution was washed with water (3 × 50 mL). Crude product was purified by flash chromatography on silica gel, eluting with EtOAc/petroleum ether 1:1 to give **12c** as a white foamy product (50 mg, yield 39%). ¹H NMR (CDCl₃, 500 MHz): δ 1.48–1.57 (m, 2H), 1.67–1.70 (m, 2H), 2.01 (s, 1H), 2.55 (tt, *J* = 3.3, 11.9 Hz, 1H), 3.03 (br t, *J* = 11.3 Hz, 2H), 4.60 (br s, 2H), 5.93 (s, 4H), 6.75 (dd, *J* = 7.6, 1.1 Hz, 2H), 6.92 (dd, *J* = 7.6, 1.5 Hz), 6.92 (s, 2H), 7.95 (s, 1H), 8.74 (s, 1H). ¹³C NMR (CDCl₃,

120 MHz) δ 151.9, 147.8, 146.5, 146.4, 144.2, 139.5, 118.8, 107.9, 106.7, 101.1, 79.3, 44.4, 38.4, 21.1.

5.1.28. 2,2,2-Trichloroethyl 4-(bis(benzo[d][1,3]dioxol-5-yl)(hydroxy)methyl)piperidine-1-carboxylate (12b)

To a solution of **15** (200 mg, 0.563 mmol) in anhydrous CH₂Cl₂ in (30 mL) was added Et₃N (0.392 mL, 2.81 mmol) and 2,2,2-trichloroethyl chloroformate (0.114 mL, 0.844 mmol), and the mixture was stirred at RT for 19 h. The reaction was quenched by addition of water. The organic phase was separated and washed with brine, and dried over Na₂SO₄. Purification by flash chromatography on silica gel column eluting with a gradient of EtOAc/petroleum ether gave white or slightly yellowish solid (210 mg, yield 70%). ¹H NMR (500 MHz, CDCl₃) δ 1.35 (qd, *J* = 12.7, 4.0 Hz, 2H), 1.60 (br s, 2H), 1.99 (s, 1H), 2.44 (tt, *J* = 11.8, 2.8 Hz, 1H), 2.76–2.95 (m, 2H), 4.26 (br s, 2H), 4.71 (q, *J* = 10.1 Hz, 2H), 5.92 (s, 4H), 6.74 (d, *J* = 7.6 Hz, 2H), 6.91 (d, *J* = 7.6 Hz, 2H), 6.92 (s, 2H). Anal. Calcd for C₂₃H₂₂Cl₃NO₇: C 52.05, H 4.18, N 2.64. Found: C 52.34, H 4.16, N 2.75.

5.2. Biological evaluation

5.2.1. Determination of MAGL activity using 2-AG as a substrate

Inhibitory activity of the synthesized compounds was determined using lysates of hrMGL overexpressing HEK cells, essentially as previously described.²⁸ The final incubation volume (100 μL) contained 2.5 μg of protein and the substrate concentration was 50 μM.

5.2.2. Determination of FAAH activity using anandamide as a substrate

Inhibitory activities of few selected compounds were determined using membranes of hrFAAH overexpressing COS-7 cells, essentially as previously described.²⁹ The final incubation volume (100 μL) contained 1 μg of protein and the substrate concentration was 20 μM (10 nM of ³H-anandamide having specific activity of 60 μCi/mmol and concentration of 1 mCi/mL).

5.2.3. Data analysis

The inhibitor dose-response curves and IC₅₀ values derived thereof were calculated from nonlinear regressions using GraphPad Prism 5.0 for Windows (GraphPad Software, San Diego California USA, www.graphpad.com).

5.2.4. Molecular modeling

Molecular modeling was performed using Schrödinger Maestro software package. Structures of small molecules were prepared using the LigPrep module of Schrodinger suite.³⁰ X-ray crystal structures for the FAAH (pdb: 3QK5)²³ and MAGL (pdb: 3PE6)¹⁴ were used for docking studies. X-ray structures were pre-processed using the protein preparation wizard of Schrödinger suite in order to optimize the hydrogen bonding network and to remove any possible crystallographic artefacts.³⁰ In the case of MAGL the grid box was centered using corresponding X-ray ligand as template and in the case of FAAH grid was centered to water molecule bound to oxyanion hole. The ligand docking was performed using default SP settings of Schrödinger Glide using hydrogen bond constraints to oxyanion hole residues (at least one contact required). Graphical illustrations were generated using MOE software (Molecular Operating Environment (MOE), 2013.8).³¹

Acknowledgements

This work was supported by the Academy of Finland (Grants 139620 to J.T.L. and 139140 J.T.N.) Biocenter Finland/DDCB

(T.L.). The authors are grateful to Mrs. Tiina Koivunen for technical assistance. CSC–Scientific Computing, Ltd is greatly acknowledged for software licenses and computational resources.

References and notes

- Cravatt, B. F.; Lichtman, A. H. *J. Neurobiol.* **2004**, *61*, 149.
- Hill, M. N.; Gorzalka, B. B. *CNS Neurol. Disord. Drug Targets* **2009**, *8*, 451.
- Savinainen, J. R.; Saario, S. M.; Laitinen, J. T. *Acta Physiol.* **2012**, *204*, 267.
- Ahn, K.; McKinney, M. K.; Cravatt, B. F. *Chem. Rev.* **2008**, *108*, 1687.
- Giang, D. K.; Cravatt, B. F. *Proc. Natl. Acad. Sci. U.S.A.* **1997**, *94*, 2238.
- Fowler, C. J.; Jonsson, K.; Tiger, G. *Biochem. Pharmacol.* **2001**, *62*, 517.
- Patricelli, M. P.; Patterson, J. E.; Boger, D. L.; Cravatt, B. F. *Bioorg. Med. Chem. Lett.* **1998**, *8*, 613.
- Kinsey, S. G.; Long, J. Z.; Cravatt, B. F.; Lichtman, A. H. *J. Pain* **2010**, *11*, 1420.
- Hill, M. N.; Hillard, C. J.; Bambico, F. R.; Patel, S.; Gorzalka, B. B.; Gobbi, G. *Trends Pharmacol. Sci.* **2009**, *30*, 484.
- Nomura, D. K.; Morrison, B. E.; Blankman, J. L.; Long, J. Z.; Kinsey, S. G.; Marcondes, M. C. G.; Ward, A. M.; Hahn, Y. K.; Lichtman, A. H.; Conti, B.; Cravatt, B. F. *Science* **2011**, *334*, 809.
- Nomura, D. K.; Long, J. Z.; Niessen, S.; Hoover, H. S.; Ng, S.; Cravatt, B. F. *Cell* **2010**, *140*, 49.
- Otrubova, K.; Ezzili, C.; Boger, D. L. *Bioorg. Med. Chem. Lett.* **2011**, *21*, 4674.
- Labar, G.; Bauvois, C.; Borel, F.; Ferrer, J.; Wouters, J.; Lambert, D. M. *ChemBioChem* **2010**, *11*, 218.
- Bertrand, T.; Augé, F.; Houtmann, J.; Rak, A.; Vallée, F.; Mikol, V.; Berne, P. F.; Michot, N.; Cheuret, D.; Hoornaert, C.; Mathieu, M. *J. Mol. Biol.* **2010**, *396*, 663.
- Schalk-Hihi, C.; Schubert, C.; Alexander, R.; Bayoumy, S.; Clemente, J. C.; Deckman, I.; Desjarlais, R. L.; Dzordzorme, K. C.; Flores, C. M.; Grasberger, B.; Kranz, J. K.; Lewandowski, F.; Liu, L.; Ma, H.; Maguire, D.; Macielag, M. J.; McDonnell, M. E.; Mezzasalma Haarlander, T.; Miller, R.; Milligan, C.; Reynolds, C.; Kuo, L. C. *Protein Sci.* **2011**, *20*, 670.
- Moreira, L.; Labar, G.; Ortar, G.; Lambert, D. M. *Bioorg. Med. Chem.* **2012**, *20*, 6260.
- Kono, M.; Matsumoto, T.; Kawamura, T.; Nishimura, A.; Kiyota, Y.; Oki, H.; Miyazaki, J.; Igaki, S.; Behnke, C. A.; Shimojo, M.; Kori, M. *Bioorg. Med. Chem.* **2013**, *21*, 28.
- Kono, M.; Matsumoto, T.; Imaeda, T.; Kawamura, T.; Fujimoto, S.; Kosugi, Y.; Odani, T.; Shimizu, Y.; Matsui, H.; Shimojo, M.; Kori, M. *Bioorg. Med. Chem.* **2014**, *22*, 1468.
- Hicks, J. W.; Parkes, J.; Tong, J.; Houle, S.; Vasdev, N.; Wilson, A. A. *Nucl. Med. Biol.* **2014**, *41*, 688.
- Aaltonen, N.; Savinainen, J.; Ribas, C.; Rönkkö, J.; Kuusisto, A.; Korhonen, J.; Navia-Paldanius, D.; Häyrinen, J.; Takabe, P.; Käsänen, H.; Pantisar, T.; Laitinen, T.; Lehtonen, M.; Pasonen-Seppänen, S.; Poso, A.; Nevalainen, T.; Laitinen, J. *Chem. Biol.* **2013**, *20*, 379.
- Katritzky, A. R.; Pleyne, D. P. M.; Yang, B. J. *Org. Chem.* **1997**, *62*, 4155.
- Chang, J.; Niphakis, M.; Lum, K.; Cognetta, A., III; Wang, C.; Matthews, M.; Niessen, S.; Buczynski, M.; Parsons, L.; Cravatt, B. *Chem. Biol.* **2012**, *19*, 579.
- Gustin, D. J.; Ma, Z.; Min, X.; Li, Y.; Hedberg, C.; Guimaraes, C.; Porter, A. C.; Lindstrom, M.; Lester-Zeiner, D.; Xu, G.; Carlson, T. J.; Xiao, S.; Meleza, C.; Connors, R.; Wang, Z.; Kayser, F. *Bioorg. Med. Chem. Lett.* **2011**, *21*, 2492.
- Käsänen, H.; Minkkilä, A.; Taupila, S.; Patel, J. Z.; Parkkari, T.; Lahtela-Kakkonen, M.; Saario, S. M.; Nevalainen, T.; Poso, A. *Eur. J. Pharm. Sci.* **2013**, *49*, 423.
- Laitinen, T.; Navia-Paldanius, D.; Ryttilahti, R.; Marjamaa, J. J. T.; Karízková, J.; Parkkari, T.; Pantisar, T.; Poso, A.; Laitinen, J. T.; Savinainen, J. R. *Mol. Pharmacol.* **2014**, *85*, 510.
- Ishii, T.; Sugane, T.; Kakefuda, A. WO Patent 2,008,023,720 A1, 2008.
- Long, J. Z.; Li, W.; Booker, L.; Burstson, J. J.; Kinsey, S. G.; Schlosburg, J. E.; Pavon, F. J.; Serrano, A. M.; Selley, D. E.; Parsons, L. H.; Lichtman, A. H.; Cravatt, B. F. *Nat. Chem. Biol.* **2009**, *5*, 37.
- Minkkilä, A.; Saario, S. M.; Käsänen, H.; Leppänen, J.; Poso, A.; Nevalainen, T. *J. Med. Chem.* **2008**, *51*, 7057.
- Saario, S. M.; Poso, A.; Juvonen, R. O.; Järvinen, T.; Salo-Ahen, O. *J. Med. Chem.* **2006**, *49*, 4650.
- Schrödinger Release 2014-1: Maestro, Version 9.7.012; Ligprep, v. 2.9; Protein Preparation Wizard: Epik Version 2.7, Impact Version 6.2, Prime Version 3.5; Glide, Version 6.2; Schrödinger, LLC: New York, NY, 2013.*
- Molecular operating environment (MOE) version 2013.8, chemical computing group Inc., 1010 Sherbooke St. West, Suite #910, Montreal, QC H3A 2R7, Canada, 2013.